J. Fluid Mech. (1970), *vol.* 42, *part* 4, *pp.* 689–699
Printed in Great Britain

A technique for phase speed measurements in turbulent flow

By G. R. STEGEN

Department of Civil Engineering, Colorado State University, Fort Collins, Colorado

AND C. W. VAN ATTA

Department of the Aerospace and Mechanical Engineering Sciences, University of California, San Diego, La Jolla, California

(Received 12 December 1968 and in revised form 20 November 1969)

A technique is described for measuring the local phase speed in a turbulent flow. The technique has been used to measure the phase speed of the Fourier components of the longitudinal velocity fluctuations in grid turbulence. These measurements are unique in that the probe spacing is only twice the Kolmogoroff length scale. The velocity fluctuations were measured with linearized constant-temperature hot-wire anemometers, the outputs of which were digitally sampled and recorded in real time. Digital Fourier analysis techniques were then used to calculate the cross-spectral density of the two velocity measurements. From this, the phase, phase speed, and coherence were calculated. The coherence has been used to estimate the variance of these measurements.

1. Introduction

It is well known that the propagation speed of velocity fluctuations in shear layers depends both on spatial location and frequency. Measurements of space-time correlations in shear flows, such as those of Fisher & Davies (1964) and Favre, Gaviglio & Dumas (1967), have led to various definitions of the apparent propagation speed. All previously reported measurements have been made at such large spatial hot-wire separations that temporal fluctuations have reduced the cross-correlation for optimum time delay to values significantly less than unity. Thus, these measurements of convection velocity were non-local in the sense that the spatial fluctuation patterns observed at both probes were not exactly the same. The preceding comments also apply to cross-correlations of the filtered signals made to determine the frequency dependence of the convection velocity.

The present paper discusses an initial attempt to define and measure a local propagation speed of Fourier components of the velocity field by comparing velocity fluctuations at two points that are separated by a distance comparable with the smallest characteristic length scales for temporal change of the fluctuations, so that the correlation between the two velocity signals is essentially unity.

Such a technique will be particularly useful in investigating free jet flows, where the propagation speed varies rapidly with distance (Stegen 1967).

1.1. *Measurement technique*

The propagation speed of fluctuations can be measured as a function of frequency by calculating the phase speed $C(f)$ from the phase difference $\phi(f)$ between the two signals,

$$C(f) = 2\pi f d/\phi(f),$$

where d is the transducer spacing in the direction of the mean flow.

This measurement is significant only if the coherence (defined in § 3.1) between the signals is high. Since the coherence is frequency dependent, this condition is stronger than requiring that the cross-correlation be high. The condition of high coherence will be satisfied if the turbulence pattern has been convected over the distance d essentially unchanged by the temporal fluctuations. In such a case we can identify $C(f)$ as the true phase speed of those Fourier components of the turbulent energy spectrum.

To determine the local propagation speed of turbulent fluctuations one should measure the phase speed with two probes separated by a distance comparable to the smallest scale of interest. For velocity fluctuations the relevant small-scale parameter is the Kolmogoroff length $L_k = (\epsilon/\nu^3)^{-\frac{1}{4}}$, where ϵ is the dissipation rate. To test the limitations of the method, the probes were spaced about $2L_k$ apart.

We chose to make these initial measurements in an unsheared, low-intensity grid-generated turbulent field to avoid some of the possible complications in interpretation noted by Lumley (1965). For this flow field we expect the phase speed to be independent of frequency. Frenkiel & Klebanoff (1966) have measured higher-order space-time correlations under similar experimental conditions. Although their second-order space-time correlations were consistent with Taylor's hypothesis, their results for higher-order correlations led them to speculate that even for grid turbulence the propagation speed may depend on the eddy size. When they compared their measured space-time correlations with one-point time correlations displaced appropriately using Taylor's hypothesis based on the mean speed, they found that odd- and even-order correlations were displaced in opposite directions from the nominal position predicted by the frozen pattern hypothesis. Reasoning that the odd-order correlations may be governed by a different range of eddy sizes (weighted toward the large eddies) from the even-order correlations, they inferred that the propagation speed might be a function of eddy size. From their limited amount of data no general trends were apparent. For example, their odd-order correlations are sometimes displaced downstream, indicating that for the particular sample of data the apparent translational velocity is smaller than U, whereas for other samples and different probe spacings the same correlations are shifted upstream, indicating a velocity somewhat greater than U.

More recently, Corrsin & Comte-Bellot (private communication) have made extensive measurements of filtered second-order space-time correlations in grid turbulence. Their results again verified Taylor's hypothesis for this flow field.

The probe spacing used here was extremely small compared to the smallest spacing ($\approx 21L_K$) used by Frenkiel & Klebanoff (1966). This results in phase

differences of only 4° at 100 Hz. The usual analogue techniques are not easily adapted to measurement of such small phase differences. Instead, the phase has been calculated from the cross-spectral density by digital techniques. The cross-spectral density was measured using the digital harmonic analysis method described by Van Atta & Chen (1968*a*). The essence of the method is to use the 'fast Fourier transform' algorithm of Cooley & Tukey (1965) to obtain the discrete Fourier transform of a sampled time series. The analysis of the data then proceeds along the usual lines of digital spectral analysis (see, for instance, Munk, Snodgrass & Tucker 1959).

2. Experimental arrangement

The experiments were carried out in the 76 cm by 76 cm by 9 m test section of the low-turbulence wind tunnel in the Department of Aerospace and Mechanical Engineering Sciences. A biplane grid of round, polished dural rods (0·953 cm diameter, mesh spacing $M = 5{\cdot}08$ cm) was located 2·4 m from the end of the contraction section. The mean velocity U was 7·7 m/sec, giving a grid Reynolds number $(UM/\nu) = 25{,}300$. All measurements were made at a downstream location $X/M = 48$, where X is the distance measured downstream from the centre of the grid. The longitudinal turbulence intensity $\sqrt{\langle u^2 \rangle}$ at this point was 1·6 % of the mean velocity.

Van Atta & Chen (1968*b*) have made quantitative measurements of the frequency range over which our example of grid turbulence can be considered locally isotropic. The energy spectrum of the transverse fluctuations (v) was compared to the spectrum deduced from the energy spectrum of the longitudinal fluctuations (u) using the isotropic relations. For the flow conditions of this experiment, they find good agreement and hence local isotropy for frequencies greater than about 80 Hz.

Conventional analogue measurement techniques were used to determine the dissipation rate $\epsilon = -\frac{1}{2}d(\langle u^2 \rangle + 2\langle v^2 \rangle)/dt$. The Kolmogoroff length scale $L_k = (\epsilon/\nu^3)^{-\frac{1}{4}}$ was 0·047 cm, and the Kolomogoroff time scale $\sigma = (\nu/\epsilon)^{\frac{1}{2}}$ was 0·0143 sec.

A special probe was built to measure u at two closely spaced locations. Two tungsten wires (0·5 mm sensitive length, 0·0038 mm diameter) were mounted parallel to each other with 0·089 cm longitudinal spacing ($\approx 2L_k$) and displaced laterally 0·0125 cm. The lateral displacement was necessary to prevent interference from the forward wire and probe tips. The wires were operated in the linearized constant-temperature mode using DISA 55A01 anemometers and DISA 55D10 linearizers. The overheat ratios were about 0·3. The linearized velocity signals were preconditioned by first removing the d.c. level, then amplifying, and finally low-pass filtering. The two signals were then simultaneously sampled and recorded on-line by an analogue-digital converter and digital tape recorder. The sampling rate for each channel was 4170 samples/second, a value sufficiently high to prevent aliasing of the energy spectrum. The frequency characteristics of the system components were carefully matched to prevent interchannel phase errors.

3. Digital cross-spectral analysis

3.1. *Phase speed calculations*

We denote two discrete time series by $x(t)$ and $y(t)$, where $t = 0, 1, \ldots, N-1$; N is the number of samples in the series.

The discrete Fourier transforms of the time series are denoted by

$$X(f) = \mathscr{F}\{x(t)\} = \Delta\tau \sum_{t=0}^{N-1} x(t) \exp(-j2\pi ft\Delta\tau),$$

$$Y(f) = \mathscr{F}\{y(t)\} = \Delta\tau \sum_{t=0}^{N-1} y(t) \exp(-j2\pi ft\Delta\tau),$$

where $f = 0, \Delta f, \ldots, (N-1)\Delta f$, $X(f)$ and $Y(f)$ are complex, and $\Delta\tau$ is the sampling interval. The frequency interval Δf of the transform is given by $\Delta f = 1/(N\Delta\tau) = 1/T$, where T is the record length.

The energy spectra are

$$E_x(f) = \overline{X(f)\,X^*(f)}/T,$$

$$E_y(f) = \overline{Y(f)\,Y^*(f)}/T,$$

where * denotes the complex conjugate, and the bar denotes the ensemble average over the realizations.

The cross-spectrum is

$$S_{xy}(f) = \overline{X(f)\,Y^*(f)}/T = C_{xy}(f) - iQ_{xy}(f),$$

where C_{xy} and Q_{xy} are the co-spectrum and the quadrature-spectrum.

The coherence R^2† and phase ϕ are given in terms of the spectra

$$R^2(f) = S_{xy}(f)\,S_{xy}^*(f)/E_x(f)\,E_y(f),$$

$$\phi_{xy}(f) = -\tan^{-1}(Q_{xy}(f)/C_{xy}(f)).$$

The phase defined in this way is the phase lead of $x(t)$ relative to $y(t)$. The phase can alternatively be written as a time delay $\tau(f)$, where

$$\tau(f) = \phi_{xy}(f)/2\pi f.$$

The coherence plays the role of a correlation coefficient defined at each frequency. It is a measure of the linear dependence of the two time series. By Schwarz's inequality, the coherence is bounded in the region $0 \leqslant R^2 \leqslant 1$. In the next section, we will see how the coherence affects the reliability of our phase estimation.

The phase speed, which is defined as

$$C(f) = 2\pi fd/\phi_{xy}(f)$$

is the apparent propagation speed of spectral components of frequency f. This definition is the same as used earlier by Lumley (1965).

3.2. *Phase errors*

Before applying the proposed technique it is important to appreciate the theoretical limitations involved in the estimates of the phase. The following discussion of phase errors is based on the assumption of Gaussianity. In grid

† Some authors prefer to call R the coherence, and R^2 the 'squared-coherence'.

turbulence the non-zero value of the triple-correlation indicates a non-Gaussian character, but the longitudinal fluctuations at a single point, and even-order two-point correlations are closely represented by Gaussian processes (Frenkiel & Klebanoff 1965; Van Atta & Chen 1968*a*).

The cross-spectral estimates of bivariate stochastic processes derived from finite length records are subject to a random error. For such Gaussian processes, the confidence limits for the phase angle ϕ_{xy} have been given by Goodman (1957). There is a probability p that the true phase will lie in the interval $\phi_{xy} \pm \Delta\phi$, where

$$\sin^2 \Delta\phi = \frac{1-R_\infty^2}{R_\infty^2}[(1-p)^{-2/\nu} - 1],$$

where ν is the number of statistical degrees of freedom and R_∞^2 is the true value of coherence. For the 'fast Fourier transform' algorithm, the value of ν is twice the number of realizations. Now, for $\nu > 200$, the 95 % confidence limits for the coherence are less than $\pm 2\,\%$ of the measured value R^2, for all values of $R^2 > 0{\cdot}80$ (Amos & Koopmans 1963). Under these conditions we can replace the true coherence R_∞^2 by the measured value R^2 with little error in our estimate of $\Delta\phi$.

The 95 % confidence limit for $\nu > 200$ reduces to

$$\Delta\phi \approx \left\{\frac{1-R^2}{R^2}\left(\frac{6}{\nu}\right)\right\}^{\frac{1}{2}},$$

where $\Delta\phi$ is in radians.

For the present data the coherence is essentially constant at low frequencies, so that $\Delta\phi$ is independent of frequency in that range. Since the phase decreases monotonically with decreasing frequency, a point will be reached where the magnitudes of ϕ_{xy} and $\Delta\phi_{xy}$ are comparable. Such a point represents a lower bound on the range of frequencies where this technique is usable.

3.3. *Influence of signal/noise ratio*

In § 3.2 we saw the key role that the coherence plays in the phase analysis. A high value of coherence is essential if reasonable estimates of the phase are to be obtained. A small probe separation was chosen to ensure that the turbulent fluctuations would be well correlated, i.e. highly coherent. However, the coherence estimate is strongly influenced by the noise superimposed on the signals. If the two signals $x(t)$ and $y(t)$ are linearly related, and if the noise signals are uncorrelated, then the coherence is given by (see, for example, Jenkins & Watts 1968)

$$R^2(f) = \frac{1}{[1+N_x^2][1+N_y^2]},$$

where N_x, N_y are the noise/signal ratios for the two signals. We see now the importance of maintaining a high signal/noise ratio if the true coherence is to be measured.

In this experiment the noise was determined by the least count error of the A–D converter at a level equivalent to 0·2 cm/sec. Consequently, the decrease in energy with increasing frequency resulted in an increase in N, and therefore a decrease in R^2. To improve the signal/noise ratio, it would suffice to increase the resolution of the A–D converter.

3.4. *Data analysis*

The data were processed on a CDC 3600 computer. The simultaneous time series were divided into 100 pairs of records, each 0·492 sec long containing 2048 data samples. The discrete Fourier transform of each record was calculated using the 'fast Fourier transform' algorithm. The frequency interval (Δf) of the Fourier transforms was 2·04 Hz. The spectra were then calculated and ensemble averaged over the 100 records (200 degrees of freedom). Next, the spectra were smoothed using a simple Hanning filter (Blackman & Tukey 1958). This operation increases the effective number of degrees of freedom by about a factor of 2, with a subsequent decrease in the variance of the phase estimate. The coherence, phase, and phase speed were then computed from the smoothed spectra. Analysis of a set of data, including plotting, required about 7 min of computer time.

4. Results

4.1. *Simulated phase shift*

In order to demonstrate the capabilities of the technique, it was first used to measure an artificial phase shift. The anticipated phase shift was simulated electronically with an analogue low-pass filter. The filter attenuation and cut-off frequency were adjusted to give a linear phase shift in the range 0–600 Hz, with a value of 24° at 600 Hz. The filter thus produced a constant time delay of 111 μsec, a good model of the 115 μsec delay expected during the experiments. The turbulence signal from one hot-wire was taken as the input: $x(t)$. This signal was then phase shifted (time delayed) with the filter to give the second signal: $y(t)$.

The coherence spectrum obtained in the simulation is shown in figure 1. The coherence is 0·99 over most of the range, as one would expect, since the filter adds very little noise in the frequency band of interest. The loss of coherence above 500 Hz is due to band-limiting of the input signal at about 600 Hz with a second low-pass filter. This decreased the signal/noise ratio, and consequently the coherence (see § 3.3). The associated phase spectrum is given in figure 2. Allowing for the statistical fluctuations, the phase varies linearly with frequency up to 500 Hz. At this point the variance of the phase increases rapidly corresponding to the drop in coherence. Equally important, the phase plot begins to depart from a linear relation at this point, indicating a bias in our estimate of the phase due to the drop in coherence.

Since we are interested in generating a constant time-delay, we have also plotted the time-delay spectrum in figure 3. The influence of statistical phase errors on the measured time delay are clearly evident here. Below 50 Hz the fluctuations overwhelm the measurement, making the technique unusable in this range. In the frequency range 100 Hz to 500 Hz the estimated time delay is about 4 μsec less the value inferred from the analogue measurement of the filter phase shift. This small time error is due to slight electronic differences in the sample and hold amplifiers used in the A–D converter. Above 500 Hz the variance increases, and the estimate is negatively biased.

From figure 3 we see that we are able to resolve time-delays considerably

smaller than the sampling interval of 250 μsec. If we were prepared to accept accuracies of $\pm$ 20 %, we could measure time delays of 20 μsec under the present conditions. At 100 Hz this corresponds to a phase shift of 0·7°, an almost impossible measurement to make by analogue methods. Herein lies the inherent advantage of the present technique. By examining the coherence and phase rather than the band-limited correlation, one can resolve very small time delays with the bonus of obtaining results over a wide range of frequencies with a single calculation.

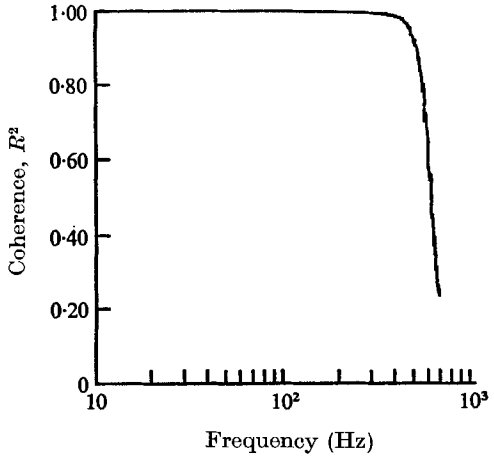

FIGURE 1. Coherence spectrum measured for two time series artificially phase shifted with an analogue low-pass filter.

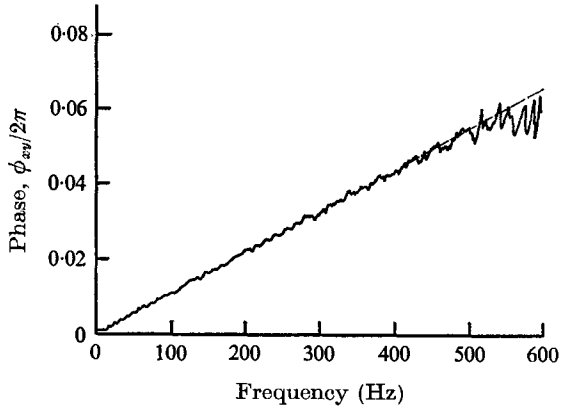

FIGURE 2. Phase spectrum measured for two time series artificially phase shifted. ———, predicted spectrum.

4.2. *Phase speed measurements*

The one-dimensional velocity spectra $E(f)$ measured by the two hot-wires are compared in figure 4. For clarity we have plotted only a few of the 1024 data points measured for each spectrum. The two spectra are practically identical,

indicating that the front hot-wire did not interfere with the rear hot-wire. However, the rear hot-wire did detect some vortex shedding from the front probe supports. The shedding frequency was 3300 Hz, well beyond the limits of the turbulent energy spectrum, and was readily removed by low-pass filtering.

The coherence (figure 5) between the two signals was quite high, as one would

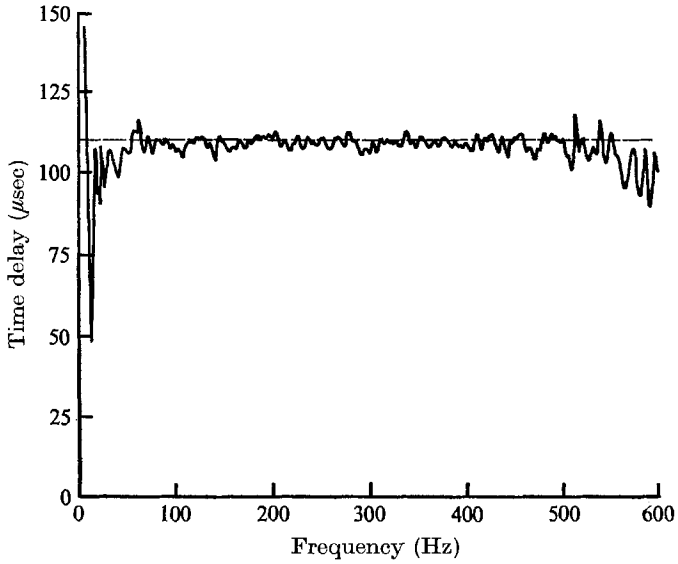

FIGURE 3. Time delay spectrum deduced from the data of figure 2. ———, predicted spectrum, $\tau = 111$ μsec.

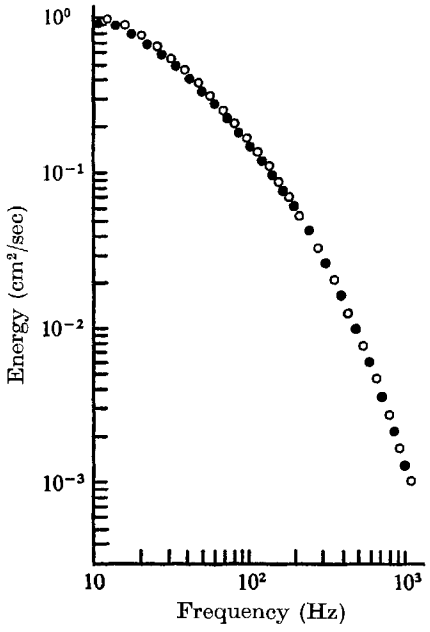

FIGURE 4. Comparison of measured one-dimensional energy spectra. ●, front hot-wire; ○, rear hot-wire.

expect at such close spacings. The maximum coherence was $\approx 0{\cdot}96$, indicating that the signals are not exactly the same. The loss in maximum coherence was primarily due to the finite resolution of the wires, whose length was only about one-half the separation distance. Strong dips are present in the coherence spectrum at the line frequencies and all higher harmonics. Close inspection of the

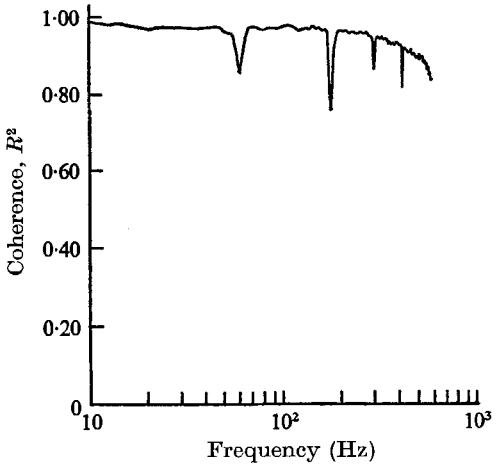

FIGURE 5. Coherence spectrum measured between two hot-wires in a turbulent flow with a streamwise separation of $2L_k$.

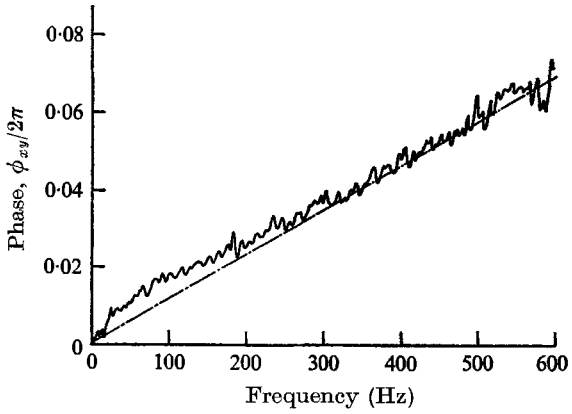

FIGURE 6. Phase spectrum measured between two hot-wires with a streamwise separation of $2L_k$. — · —, value predicted at the mean speed. The data shown is a computer generated plot of 294 data points with a frequency interval of 2·04 Hz.

computed spectra indicated that one signal had an excessive amount of 60 Hz noise. This resulted in a locally reduced signal/noise ratio, which apparently accounts for the loss of coherence at 60 Hz and its harmonics. The coherence drops to $\approx 0{\cdot}85$ at 600 Hz, due to the decrease in signal-to-noise ratio as the energy spectrum falls off.

The measured phase spectrum is shown in figure 6. We note a marked increase in the variability of ϕ_{xy} as compared to the artificial phase shift case, a consequence of the reduced coherence. More significant is the deviation from the

expected curve at frequencies below 300 Hz. This was at first interpreted as implying that the low frequencies propagate at less than the mean speed (Stegen & Van Atta 1968), a result in conflict with the conclusions of earlier investigators.

As indicated earlier, great care was taken to prevent electronic phase errors. As a final check on the system, two wires were arranged in the same longitudinal plane, parallel, and laterally spaced 0·089 cm apart. Measurements of the phase spectrum for this configuration indicated a relative phase shift between the two anemometers in the frequency range 0–300 Hz. The time error inferred from the phase spectrum had a maximum value of about 40 μsec. This small difference would represent a negligible error for most anemometer measurements. The time delay is due to small electronic differences between the two anemometers. However, we were unable to determine exactly where in the anemometers the mismatch occurs.

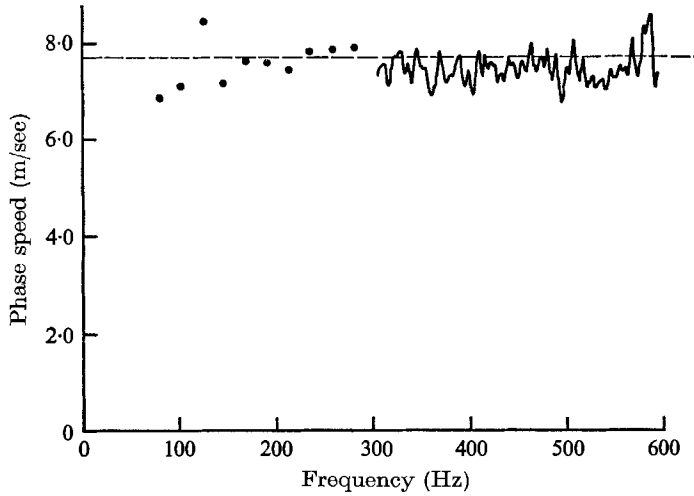

FIGURE 7. Phase speed spectrum deduced from the data of figure 6. ●, data corrected for electronic mismatch of anemometer systems. ———, mean speed, U = 7·7 m/sec.

To complete the demonstration of the technique, the measured anemometer time delay errors were used to correct the experimental data. The final measured phase speed spectrum is given in figure 7. The single points represent the corrected data, where the value has been averaged over a band 22·4 Hz wide. Because of the large uncertainty at low frequencies, no data is presented in the range 0–80 Hz. Above 300 Hz the uncorrected data was plotted every 2·0 Hz as originally calculated. The data indicates an average phase speed of 7·4 m/sec, compared to the mean speed of 7·7 m/sec. If we also account for the time errors introduced by the A–D converter, the average phase speed agrees with the mean speed within $\pm$ 1 %.

The present measurements are a systematic extension of the Fourier analysis techniques used to determine the energy spectrum of the velocity fluctuations. The measured phase speed is the propagation speed which can be associated with each frequency in the energy spectrum. We emphasize that this interpretation is valid only in the frequency range where the coherence remains high. The results

clearly demonstrate the validity of the technique. The variance of the estimate for this case is a little high for general application. However, the variance could be reduced to less than 4 % by optimizing the statistics and probe configuration for a particular flow field.

5. Summary

Digital harmonic analysis employing the fast Fourier transform algorithm has provided an efficient means for measuring very small phase shifts between two time series. Using digital methods, a technique for measuring local phase speeds in turbulent velocity fields has been developed. In developing the technique, we have drawn heavily upon the similar work by Munk, Snodgrass & Tucker (1959) in ocean waves. This study has emphasized the theoretical and practical considerations which limit the application of the technique.

The authors would like to thank Mr W. Y. Chen for his help with the computer programming and Professor R. A. Haubrich for his insight into bivariate stochastic processes. We also thank a reviewer of the original manuscript, whose comments helped us to discover a source of error in the phase measurements at low frequencies.

These studies have been supported at the University of California, San Diego under Project THEMIS, sponsored by the Air Force Office of Scientific Research, under Contract F44620-68-C-0010; and at Colorado State University under Project THEMIS, sponsored by the Office of Naval Research under Contract number N0014-68-A-0493-0001, Project number NR062-414/6-6-68 (Code 438) United States Department of Defense.

REFERENCES

Amos, D. E. & Koopmans, L. H. 1963 *Sandia Corporation Monograph*, SCR-483.

Blackman, R. B. & Tukey, J. W. 1958 *The Measurement of Power Spectra*. New York: Dover.

Cooley, J. W. & Tukey, J. W. 1965 *Math. of Comput.* **19**, 297.

Favre, A., Gaviglio, J. & Dumas, R. 1967 *Phys. Fluids Suppl.* **10**, S138.

Fisher, M. J. & Davies, P. O. A. L. 1964 *J. Fluid Mech.* **18**, 97.

Frenkiel, F. N. & Klebanoff, P. S. 1965 *Phys. Fluids*, **8**, 2291.

Frenkiel, F. N. & Klebanoff, P. S. 1966 In *Dynamics of Fluids and Plasmas*. New York: Academic.

Goodman, N. R. 1957 *Sci. Paper* 10, Engng Stat. Lab. New York University.

Jenkins, G. M. & Watts, D. G. 1968 *Spectral Analysis and its Applications*. San Francisco: Holden-Day.

Lumley, J. L. 1965 *Phys. Fluids*, **8**, 1056.

Munk, W. H., Snodgrass, F. E. & Tucker, M. J. 1959 *Bull. Scripps Inst. Oceanog. Univ. Calif.* **1**, 283.

Stegen, G. R. 1967 Dissertation, Stanford University.

Stegen, G. R. & Van Atta, C. W. 1968 *Bull. Am. Phys. Soc.* **13**, 1585.

Van Atta, C. W. & Chen, W. Y. 1968*a* *J. Fluid Mech.* **34**, 497.

Van Atta, C. W. & Chen, W. Y. 1968*b* *J. Fluid Mech.* **38**, 743.